A NOVEL OPTICAL GRANULOMETRY ALGORITHM
FOR ORE PARTICLES

Y. Junhao[#*], Z. Xiubin[*] and Q. Jie[*]

[*]Shanghai Jiao Tong University, School of EE, Shanghai 200240, China

Abstract

This paper proposes a novel algorithm to detect the particle size distribution of ores with irregular shapes and dim edges. This optical granulometry algorithm is particularly suitable for blast furnace process control, so its result can be used directly as a reliable basis for control system dynamics optimization. The paper explains the algorithm and its concept, as well as its method, which consists of five steps to detect ore granularity and distribution. A series of comparative experiments under industrial environments proved that this novel algorithm, compared with conventional ones, improves the accuracy of granulometry.

Keywords: Particle Size Distribution; Optical Granulometry; Double Circle; Planar Subdivision; Region Expansion; Computer Vision.

1. Introduction

During the feeding process of a blast furnace, raw materials should be uniformly distributed in accordance with their granularity, so as to ensure the quality of the process [1, 2]. In order to make a blast furnace more effective, granulometry measurements are taken first to obtain a reliable basis for the associated control system dynamics optimization.

Compared with traditional granulometry methods such as an artificial screen, optical methods have more advantages. They are non-contact in operation, which will not disturb the industrial process to make results closer to an actual situation. They can also measure the distribution across the whole

---

[#] *Corresponding author: enjoysoft@sjtu.edu.cn*

surface and are not limited to the part under the screen. Today, more and more optical granulometry algorithms to obtain the granularity of ore particles are being introduced into blast furnace process control.

While taking optical granulometry measurements, a special camera device acquires surface pictures of the ore. Particle size distribution (PSD) [3] should be calculated inside certain zones of the surface, so as to guide the control system to make better decisions, and then adjust the feeding devices to achieve the optimized aim automatically.

It is clear that the optical granulometry algorithm is the key technology for the entire system. Faced with poor illumination and the dusty environment inside a blast furnace, many conventional algorithms may fail to get accurate results. This paper proposes a better algorithm to resolve such problems.

2. Basic concepts

Optical granulometry is traditionally an image segmentation problem. Commonly-used image segmentation techniques are mainly divided into four categories: thresholding, edge division, clustering and texture analysis [4]. Conventional algorithms using these techniques in other areas are usually applied to simple situations, such as biological or chemistry particles with large contrasts between the background and the regular geometry shapes. Since the ore surface is not a typical scenario with a background and foreground, thresholding is not suitable. All ore particles are of a similar pattern and texture, and clustering and texture analysis cannot be used to separate

them. Edge division is the only starting point for doing optical granulometry on ore particles.

Figure 1 shows part of a picture taken from an ore surface in the blast furnace during the ore feeding process. From the picture, we can see that, in general, raw materials of the industrial process are irregular shapes. They have thousands of different sizes and shapes, one overlaps another, and the edges of particles are dim and obscure due to a rather thick layer of dust over them and lack of illumination.

Most conventional methods focus on how to retrieve the exact and accurate contour of each particle. These contours are sufficient for calculating the ore particle size. However, due to the above mentioned environmental conditions, satisfactory results are usually not practically available. An alternative approach being considered is to find the actual centroid position of each particle instead of its contour. Since particles usually cluster together, the distances between them can statistically decide the ore PSD.

Fig. 1 A surface view of blast furnace particle distribution

The algorithm in this paper first calculates the centroid position for each particle based on the detected edges, and uses several methods to overcome the wrongly classified fake edges. Delaunay planar division is used to expand the regions occupied by particles, in order to reflect the distances between particles. The "double circle" of each particle region, meaning the smallest circumscribed circle and the largest inscribed circle, is then retrieved. Finally, the radiuses of the two circles based on the shape analysis are used to automatically identify the particle's granularity. The formula for calculating the granularity is as follows:

$$d = R \cdot T \left[\frac{R}{r}, 2 \right] \qquad ...(1)$$

where R and r are the radiuses of the smallest circumscribed circle and the largest inscribed circle, respectively. $T[.]$ can be any type of T-norm fuzzy logic operator [5], to make sure that the supremum of granularity does not exceed the diameter of region's smallest circumscribed circle, or $d \le 2R$.
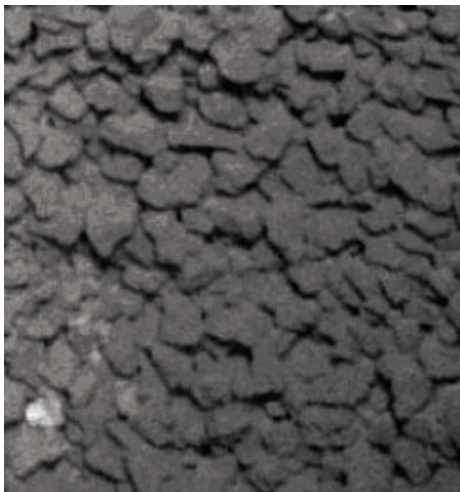
Fig.2 Preprocessing result of Fig.1

3. Algorithm steps

The algorithm consists of the following five steps: image pre-processing, morphological smoothing, positioning of particle points, region expansion of particles, double circle granularity detection.

3.1. Image Pre-processing

The image shown in Figure 1 is first converted from RGB space into HSV space [6], whose three components indicate hue, brightness and saturation. Each component is pre-processed through a Gaussian smoothing filter and histogram equalization, to enhance the image's quality as well as reduce noise. Figure 2 shows the preprocessed result of Figure 1.

3.2. Morphological smoothing

In order to restore the scattered edges caused by shadows and reflections, further smoothing is used to separate the particles. Smoothing here does not mean space or frequency domain filters, since they will ruin the edges. Instead, we use the color morphology method as the smooth operator. This method inherits the mathematical basis of the binary and grayscale morphology [7], and can be used to merge image pixels with close hue, brightness or stature. In order to understand the issues, we use the hue component H as an example, described as follows:

First, select a morphology structure element $B=B(x,y)$, such as circle of radius 5 pixels, where x and y are the coordinates of the image.

Secondly, use the hue component $H=H(x,y)$, of image at pixel (x,y), and do the grayscale dilate operation $H \oplus B$ defined as:

$$(H \oplus B)(x,y) = \max\{H(s-x,t-y) +$$
$$B(s,t)|(s-x,t-y) \in D_H \, and \, (s,t) \in D_B\} \quad ...(2)$$

Then, use the same B to do the erode operation $H \ominus B$ as:

$$(H \ominus B)(x,y) = \min\{H(s+x,t+y) -$$
$$B(s,t)|(s+x,t+y) \in D_H \, and \, (s,t) \in D_B\} \quad ...(3)$$

D_H and D_B in formula (2) and (3) are domains of H and B.

Thirdly, combine the dilate and erode operations, and do the open and close operations as follows:

Open: $H \otimes B = (H \oplus B) \ominus B$ ...(4)

Close: $H \odot B = (H \ominus B) \oplus B$ ...(5)

Repeat the open and close operations on the saturation component S and the brightness component V. Merge the above three smoothed components into an HSV image. Then do the inverse conversion from
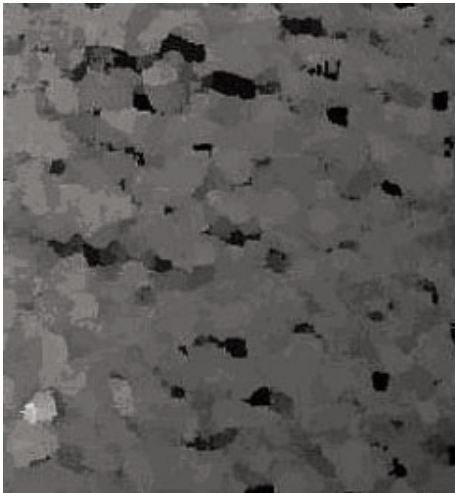
Fig. 3 Morphology smoothing result of Fig.2

HSV space to RGB space to generate a new image. Figure 3 shows the morphology smoothing result of Figure 2. From the figure, we can see that the color granulation of particles is evident. All particles are segmented into different color blocks, which is helpful for the following edge detection.

3.3. Positioning of particle points

To identify the exact granularity of particles, we use the improved color space Canny algorithm [8, 9] to extract the edges of the smoothed image in Figure 3. The extracted edges are shown in Figure 4 as white lines. It can be seen from Figure 4 that there are still some pixels that are wrongly classified as edge points due to the noise, dust or dim illumination. These fake edge points must be filtered out after edge extraction. To accomplish this, the window projection method can be used.

The window projection method means setting a window with adjustable size to scan the entire image. The window size determines the detectable granularity of particles. It must be larger than the gap size between particles and smaller than the minimum detectable granularity. We can predetermine the window size according to granularity of ore from experience. We scan the entire image and count the number of edge points inside the window using formula (6):

$$r(m,n) = \sum_{x=m-s/2}^{m+s/2} \sum_{y=n-s/2}^{n+s/2} f(x,y) \qquad ...(6)$$

where, *f(x,y)* is the extracted binary edge image with edge pixels of value 1 and non-edge pixels of value 0; x and y are the

image's abscissa and ordinate; s is the adjustable window size; m and n are the center of the scanning window; $r(m,n)$ is the count of edge points inside window.

Compare $r(m,n)$ with an adjustable threshold, from experience usually with a strong relationship with the particle surface areas. If the total number of edge points inside a window is less than this threshold, the point at the window center will be considered as a non-edge point. The white regions shown in Figure 4 are made of non-edge points from Figure 3.

$$\begin{cases} c_x = \dfrac{\sum\limits_x \sum\limits_y x \cdot g(x,y)}{\sum\limits_x \sum\limits_y g(x,y)} \\ c_y = \dfrac{\sum\limits_x \sum\limits_y y \cdot g(x,y)}{\sum\limits_x \sum\limits_y g(x,y)} \end{cases} \quad ...(7)$$

in which, $g(x,y)$ is the separate binary region image, with the inside pixels of value 1, and the outside pixels of value 0; c_x and c_y are the calculated coordinates of this region's centroid. In Figure 5, white spots indicate the calculated positions of particles in Figure 1.
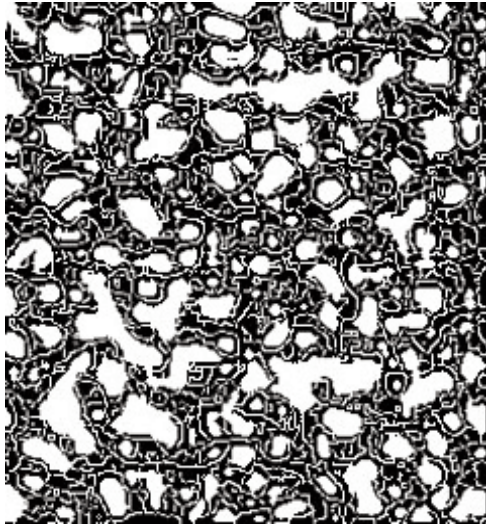
Fig. 4 Extracted edge and region detection result of Fig. 3
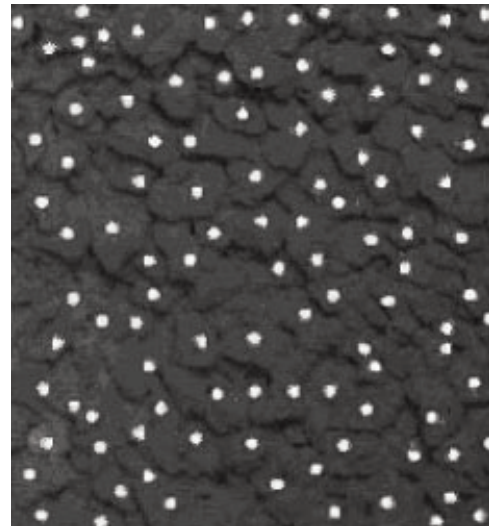
Fig. 5 Centroid position of Fig. 3

On the other hand, we can further determine the actual positions of particles in order to keep track of particle numbers and locations. A particle region may contain more than one non-edge point, such as the simply connected regions shown in Figure 4. We use a binary contour extraction algorithm to divide this binary image into separate simply connected regions. The particle position can be treated as the centroid of each region, as shown in formula (7):

3.4. Region expansion of particles

Using particle positions from the previous step, we expand the regions of particles with the help of planar subdivision. As an example, we use the improved Delaunay-Voronoi algorithm to divide the ore surface plane into regions. The result is shown in Figure 6. The black spots in the figure are the position points of particles from Figure 5.

The gray block around each spot forms the largest expansion region. Points inside each spot's block are nearer to this spot than all the other spots. It is clear that the points on black borders are equidistant with two or more particles.

It should be emphasized that the expansion regions are not identical with the particles' occupied regions, but they still have statistical significance. The region will be used by the double circle algorithm to decide the particle size distribution statistically.

It must be pointed out that the classic Delaunay triangular algorithm [10] is based on discrete grids with theoretical uniqueness and rigor, and can meet the empty-circle criterion. However, it is not easy to introduce new typical lines and is slow when building a large mesh grid. If the point set makes non-convex regions or contains inner loops, it will generate illegal triangles.

In order to overcome these shortcomings, this paper adopts an improved algorithm to enhance the division efficiency, although this algorithm relaxes the constraint of the empty-circle criterion.

3.5. Double circle granularity detection

This final step of shape analysis is divided into three substeps:

First, find the smallest circumscribed circle of a particle's expansion region using three contact vertexes. This circle is the smallest circle which contains all the pixels inside the region. In Figure 7, circle O_{abc} is the smallest circumscribed circle of the central region, in which a, b and c are chosen as the appropriate contact vertexes;

Secondly, find the largest inscribed circle of this particle's expansion region using three tangent edges. This circle is the largest circle which only contains the pixels inside the region. In Figure 7, circle O_{efg} is the largest inscribed circle of the central region, in which e, f and g are chosen as the appropriate tangent edges;

Finally, calculate the radiuses of both the smallest circumscribed circle and the largest
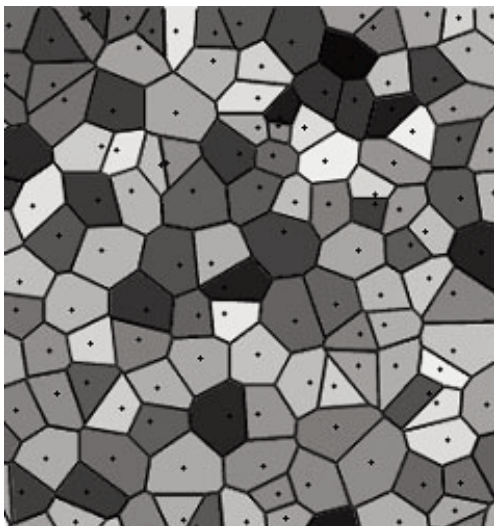
Fig. 6 Particles expansion results of Fig. 5
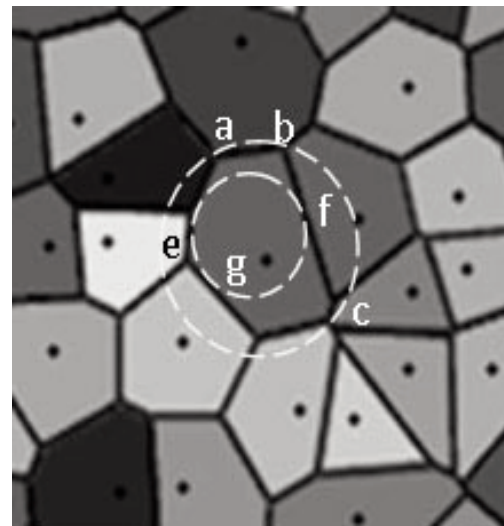
Fig. 7 Double circle ratio illustration

inscribed circle and put them into formula (1) to get granularity *d*.

After the above five steps from 3.1 to 3.5, we may further filter out the fake regions. Exclude some unreasonable regions such as small fake regions due to dust, small gap and noise, or large fake regions due to the barriers, calibrations and reflection.

4. Experiments

4.1. Study cases

To validate the algorithm proposed in this paper, we take pictures of the ore surfaces during feeding process of a blast furnace in a large-scale steel plant. Since we use the optical granulometry as a basis for feeding control system optimization, we divide the surface into eight radial zones from the interior wall to the center of the blast furnace. In order to be consistent with artificial screen mesh size, we set the following classification criteria: *d ≤ 15 mm, 15 mm < d ≤ 25 mm, 25 mm < d ≤ 40 mm, 40 mm < d ≤ 55 mm* and *d > 55 mm*, in which *d* is the diameter size of ores.

We apply the conventional algorithm using the image threshold and edge segment, provided by reference [3]. We also calculate the ore granularity using the novel algorithm proposed in this paper. We calculate the particle size distribution as follows:

$$\eta_{ij} = \frac{\alpha_{ij}}{\beta_i} \times 100\% \qquad ...(8)$$

where η_{ij} is the distribution percentage, α_{ij} is the number of class *j* (*j=1,2,....,5*) particles inside zone *i* (*i=1,2,....,8*), and β_i is the total number of the five classes of particles inside zone *i*.

4.2. Results

We filter the ores through screens and do the artificial statistics. We compare the experimental results of the two algorithms along with the statistics from the artificial screens. The results are shown in Table 1 ~ 3.

Table 1. Results of Novel Algorithm

Zones	Particle Size Distribution in zones (%)				
	≤15mm	15mm ~25mm	25mm ~40mm	40mm ~55mm	> 55mm
1	2.17	6.62	16.12	35.07	40.03
2	5.44	8.8	6.94	39	39.85
3	3.18	4.3	10.72	39.37	42.44
4	3.69	6.46	2.74	41.36	45.79
5	3.79	6.25	6.86	29.55	53.61
6	1.06	2.84	10.09	25.26	60.75
7	3.68	5.56	3.69	23.54	63.56
8	4.79	4.57	6.93	20.49	63.29

Table 2. Results of Comparison algorithm

Zones	Particle Size Distribution in zones (%)				
	≤15mm	15mm ~25mm	25mm ~40mm	40mm ~55mm	> 55mm
1	3.72	5.91	15.33	35.82	39.22
2	4.64	6.71	6.83	41.5	40.17
3	1.66	5.17	11.52	37.59	44.12
4	3.32	5.22	5.47	40.73	45.34
5	5.33	7.4	5.52	30.53	51.32
6	0.56	3.36	9.2	23.64	63.3
7	1.79	7.29	4.01	21.56	65.42
8	5.27	4.3	8.12	20.34	62.06

Table 3. Results of Artificial tests

Zones	Particle Size Distribution in zones (%)				
	≤15mm	15mm ~25mm	25mm ~40mm	40mm ~55mm	> 55mm
1	2.2	6.15	15.96	36.63	39.13
2	5.08	9.41	6.9	39.87	38.79
3	3.92	3.24	9.97	39.53	43.33
4	2.81	6.31	1.95	42.8	46.13
5	2.29	5.35	8.55	29.86	53.99
6	0.74	2.73	9.92	25.62	60.93
7	2.4	7.03	3.9	23.73	62.89
8	4.61	4.98	7.34	20.61	62.42

4.3. Error analysis

The average errors of the two algorithms could be evaluated either by zone or by class. See error graphs in Figures 8 and 9. Through these tables and figures, we can see that the maximum, minimum and average errors of the novel algorithm are smaller than the comparison algorithm by 0.84%, 0.20% and 0.60%, respectively.
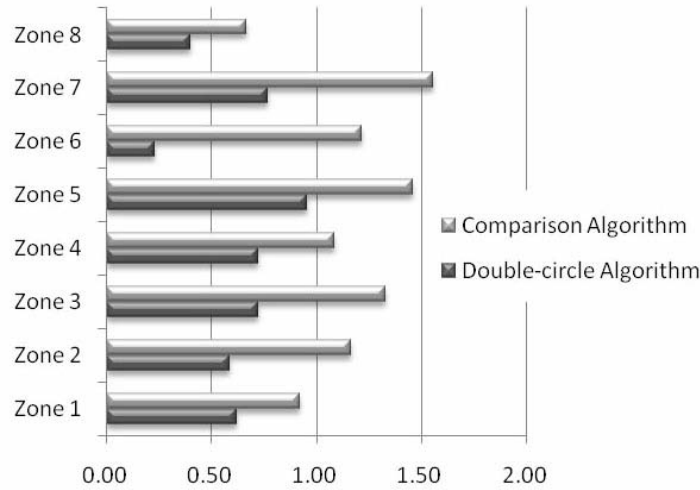
Fig. 8. Average error comparison by zones
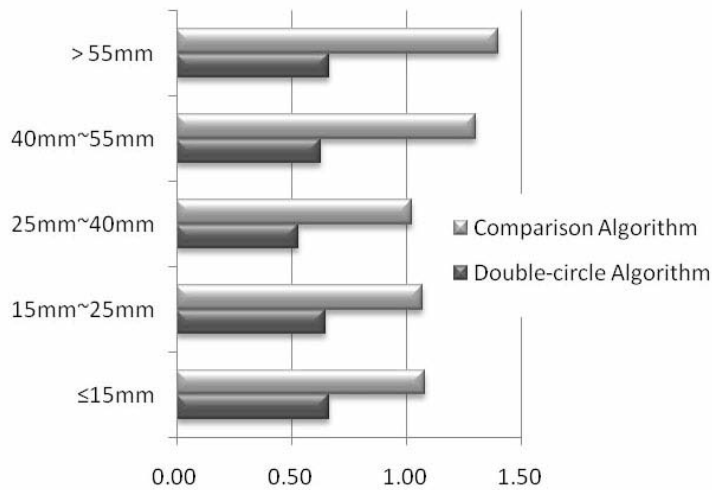
Fig. 9. Average error comparison by classes

5. Conclusion

This paper proposes an optical granulometry algorithm for irregular ores with dim and obscure edges. According to the above experiments, the concept of double circle ratio has given the algorithm evident superiority and practicality over the conventional ones. Experiments in the large-scale steel plant validated and affirmed the fact that it is particularly suitable for feeding process control optimizations of blast furnaces as well as other particle size distribution measurement systems. The idea of region expansion and double circle ratio is also instructive to other optical measurement systems.

References

[1] B. Taraba, V. Slovak, Z. Michalec, J. Chura, A. Taufer, Journal of Mining and Metallurgy Section B-Metallurgy, 44 (1) B (2008) 73.

[2] B. Trumic, D. Stankovic, V. Trujic, Journal of Mining and Metallurgy Section B-Metallurgy, 45 (1) B (2009) 79.

[3] A. Jillavenkatesa, S.J. Dapkunas, L.S. Lum, Particle Size Characterization, NIST Special Publication, 960-1, 2001

[4] L.G. Shapiro, G. Stockman, Computer Vision. New Jersey, United States: Addison Wesley, 2005

[5] W. Lixin, A Course In Fuzzy Systems & Control, United States: Pearson Education, June, 2003

[6] A.Ford, A. Roberts. Color Space Conversions 1998, www.poynton.com/PDFs/coloureq.pdf.

[7] J. Serra Image analysis and mathematical morphology. London: Academic Press, 1982

[8] J. Canny. A Computational Approach to Edge Detection, IEEE Trans. on Pattern Analysis and Machine Intelligence, 8 (6) (1986) 679.

[9] Lindeberg, Tony, Edge detection and ridge detection with automatic scale selection, International Journal of Computer Vision, 30 (2) (1998) 117.

[10] A. Aggarwal, L.J. Guibas, J. Saxe, and P.W. Shor, A linear-time algorithm for computing the Voronoi diagram of a convex polygon, Discrete Comput. Geom., 4 (6) (1989) 591.